JACS
JOURNAL OF THE AMERICAN CHEMICAL SOCIETY

ARTICLE

pubs.acs.org/JACS

# Size-Dependent Reactivity in Hydrosilylation of Silicon Nanocrystals

Joel A. Kelly,[†] Amber M. Shukaliak,[†] Michael D. Fleischauer,[‡] and Jonathan G. C. Veinot*[,†]

[†]Department of Chemistry, University of Alberta, Edmonton, Alberta T6G 2G2, Canada

[‡]NRC-National Institute for Nanotechnology, Edmonton, Alberta T6G 2M9, Canada

Supporting Information

**ABSTRACT:** We present an investigation into the influence of nanocrystal size on the reactivity of silicon nanocrystals (Si-NCs) in near-UV photochemical hydrosilylation. The size-dependent reactivity of Si-NCs with photoluminescence (PL) in the visible and near-infrared regions was evaluated using PL and Fourier-transform infrared (FTIR) spectroscopy, and small-angle X-ray scattering (SAXS). Under near-UV excitation, Si-NCs with PL in the visible spectral region react faster than Si-NCs with near-IR PL, allowing partial separation of a mixture of Si-NC sizes through hydrosilylation. This is attributed to quantum size effects in the exciton-mediated mechanisms proposed for this reaction.

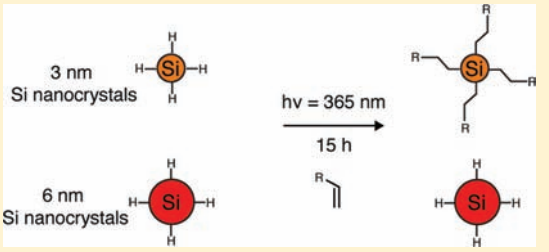


## INTRODUCTION

Interest in the chemical modification of hydride-terminated silicon surfaces has grown rapidly since the first report of hydrosilylation of a bulk Si surface by Linford and Chidsey.[1] Functionalization of bulk and nanostructured surfaces is a critical step in many envisioned applications where control over the chemical, physical, and electronic properties of the Si surface is required. Among the various methods used to functionalize Si surfaces, hydrosilylation produces high quality, densely packed organic monolayers under relatively mild reaction conditions and provides excellent stability against oxidation.[2−6]

Despite the growing number of publications on surface hydrosilylation, uncertainty regarding the mechanism(s) responsible has remained. The first reports of hydrosilylation with bulk surfaces utilized a peroxide initiator (i.e., ROOR′);[1] subsequently, hydrosilylation was shown to occur in the absence of a chemical initiator under photochemical[7,8] or thermal conditions.[9,10] Scanning tunneling microscopy (STM) studies of bulk surfaces suggested a radical propagation mechanism,[11,12] analogous to the free radical process proposed for *tris*-(trimethylsilyl)silane by Chatgilialoglu and co-workers.[13]

The pathway(s) through which this reaction is initiated has been an ongoing issue of debate; direct homolysis of a surface silicon-hydride bond under thermal or photochemical energy has been suggested in some cases, although this is not fully consistent with reports of hydrosilylation under conditions insufficient for direct cleavage of surface hydrides. Several alternate theories have been proposed, including initiation from trace molecular oxygen,[14] alkyl radicals produced by photolysis[15] or thermal olefin decomposition,[16] and the involvement of excitons (vide infra). Nonradical mechanisms under certain conditions have also been proposed, including deep-UV photoemission,[17] fluoride-assisted nucleophilic attack (due to residual $F^-$ from hydrofluoric acid etching),[18] and concerted addition under thermal conditions.[19]

Exciton-mediated mechanisms for hydrosilylation have received substantial attention for reactions performed under very mild reaction conditions, using visible light (i.e., far below the threshold for direct hydride homolysis) as an initiator,[20,21] or even for formation of self-assembled monolayers in the dark at room temperature.[22,23] Stewart and Buriak proposed a nonradical exciton-mediated mechanism holding exclusively for nanostructured Si, involving nucleophilic attack from the olefin at a surface-localized hole.[20] Subsequently, Zuilhof and co-workers observed monolayer formation on bulk surfaces by visible light.[21] On the basis of a dopant dependence and STM measurements demonstrating island growth,[24] they proposed a radical mechanism whereby delocalized holes susceptible to nucleophilic attack from the incoming olefin initiate radical propagation (analogous to the free radical mechanisms originally proposed). The involvement of delocalized excited states in these reactions is fascinating, for it has no obvious molecular counterpart; for example, while the molecular silylium ion ($R_3Si^+$) exhibits transient stability,[25] these mechanisms invoke such species as long-lived intermediates on the basis of enhanced back-bonding from surrounding lattice Si atoms. The exciton-based nanoscale and bulk mechanisms are compared to the free radical mechanism in Scheme 1.

Theoretical studies of visible light initiated hydrosilylation reactions have also given evidence for the involvement of excitons. Using model Si clusters reacting with ethene, Reboredo et al. calculated energy barriers for the reaction with the cluster in the ground (singlet) and excited (triplet) state at the DFT level of theory (following path B in Scheme 1).[26] The excited state reaction was predicted to involve a metastable intermediate state, lowering the activation energy for Si−C bond formation.

**Received:** March 20, 2011
**Published:** May 19, 2011

ACS Publications © 2011 American Chemical Society



dx.doi.org/10.1021/ja2025189 | *J. Am. Chem. Soc.* 2011, 133, 9564–9571

**Scheme 1. Depiction of the Proposed (a) Free Radical Mechanism under Thermal and Photochemical Conditions (Involving Direct Hydride Homolysis),[7,9,10] (b) Exciton-Mediated Mechanism for Nanoscale Si under Photochemical Conditions,[20] and (c) Exciton-Mediated Mechanism for Bulk Si under Photochemical Conditions[21]**

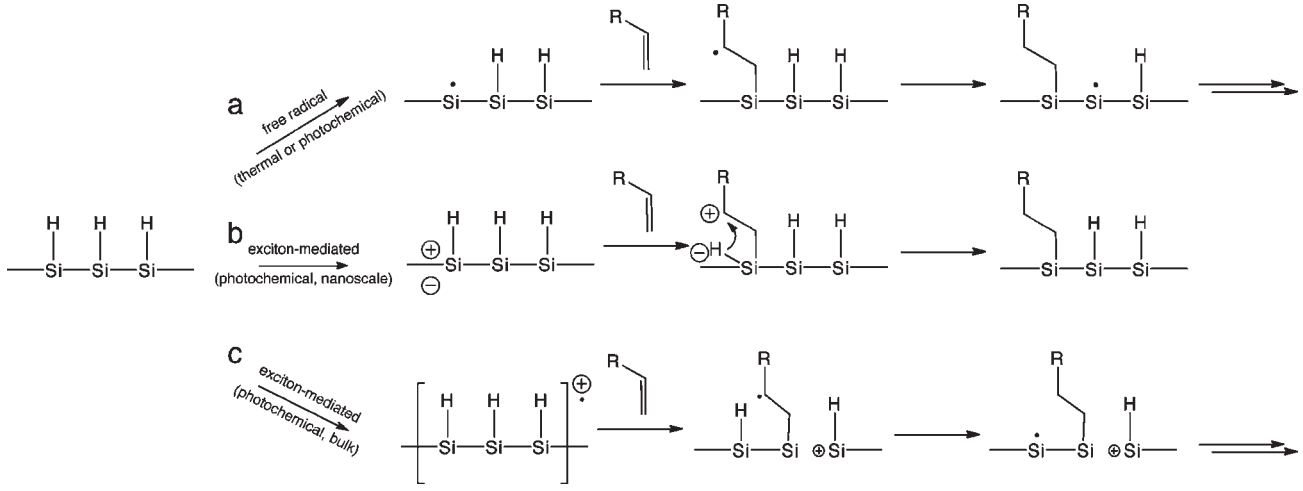


Interestingly, they proposed a rationale for differences in reactivity based upon size; as a localized midgap state, the energy of the intermediate state was found to be independent of cluster size. However, the energy of the cluster in the excited state was predicted to depend upon size, decreasing with larger size (as expected for quantum confinement effects). Thus, smaller Si nanostructures were predicted to be more reactive in this mechanism. Subsequently, Kanai and Selloni investigated the exciton-mediated mechanism on bulk surfaces (path C in Scheme 1),[27] suggesting radical chain propagation from a neighboring surface hydride may have a lower activation barrier than abstraction from the Si−C bound surface atom, in keeping with the experimental results of Zuilhof and co-workers.

For nanostructured Si (including silicon nanocrystals, Si-NCs) exhibiting intense size-dependent photoluminescence (PL) through the influence of quantum confinement effects,[28] the chief goals of functionalization through hydrosilylation are to protect the surface against oxidation (which has been implicated in shifting/quenching Si-NC PL)[29,30] and ensure colloidal dispersity in a range of solvents (especially biological/aqueous conditions, as Si-NCs have garnered much interest as biocompatible quantum dots for *in vivo* imaging).[31−35] Yet, depending on their desired application, further requirements (e.g., incorporation of a $\omega$-substituted bioactive moiety) may complicate the choice of reaction conditions used to modify Si-NC surfaces. For example, a recent interest in the functionalization of compound II−VI and III−V semiconductor NCs (e.g., CdSe, GaAs) has been the development of surface ligands that do not hinder thin-film conductivity (either through a postreaction treatment to remove the insulating alkyl chains from the as-synthesized materials,[36,37] or through use of novel inorganic ligands[38]) for devices utilizing their quantum confined optical and electronic properties. The use of shorter alkyl chains is incompatible with the reported temperature requirements of thermal hydrosilylation (ca. 120−200 °C), and some olefins decompose under deep-UV irradiation.[39] Furthermore, several functional groups compete for addition to hydride-terminated Si surfaces (e.g., amines,[40] halides,[41] and nitro moieties[42]). It is therefore important to understand the mechanistic considerations that might limit reactivity for a given Si-NC size, alkene or alkyne, and method of initiation desired.

We previously investigated the use of near-UV light to initiate hydrosilylation using Si-NCs with PL in the visible region (e.g., sizes of ca. 1.5−3 nm).[30] The irradiating wavelength of 365 nm was chosen as this corresponds to a region of direct-gap light absorption, which might enhance the rate of reaction in the exciton-mediated mechanisms (i.e., paths B and C in Scheme 1). Si-NCs were prepared through the thermal decomposition of hydrogen silsesquioxane (HSQ).[43,44] This synthesis yields size-controlled Si-NCs with a relatively narrow polydispersity, making it well-suited for a fundamental investigation into size-dependent reactivity. Here, small-angle X-ray scattering (SAXS), photoluminescence (PL), and Fourier transform infrared (FTIR) spectroscopy have been employed to experimentally investigate the reactivity of Si-NCs as a function of size in near-UV hydrosilylation. The size ranges selected (ca. 2−3 nm Si-NCs with PL centered at ca. 700 nm, referred to as "small" NCs in the text and ca. 5−7 nm Si-NCs with PL centered at ca. 950 nm, referred to as "large" NCs in the text) were chosen as these populations are near the Bohr radius of Si of ca. 5 nm, the threshold where quantum size effects that might impact the hydrosilylation are expected to arise.[28] The present results demonstrate "large" Si-NCs react at a slower rate than "small" Si-NCs under near-UV hydrosilylation, allowing a mixture of the two populations to be partially size-selected based upon their reactivity. This difference in reactivity is suggested to arise due to the impact of quantum confinement effects on the exciton-mediated mechanisms,[20] and is consistent with the theoretical predictions made by Reboredo et al.[26]

## RESULTS AND DISCUSSION

A natural extension of our investigation of near-UV hydrosilylation using Si-NCs with PL in the visible region is the functionalization of larger Si-NCs with PL in the near-IR (i.e., 700−1100 nm). This spectral region is of particular interest for application in biological imaging, as it occurs in the therapeutic window where light maximally penetrates tissue.[45] Si-NCs with


dx.doi.org/10.1021/ja2025189 |*J. Am. Chem. Soc.* 2011, 133, 9564–9571

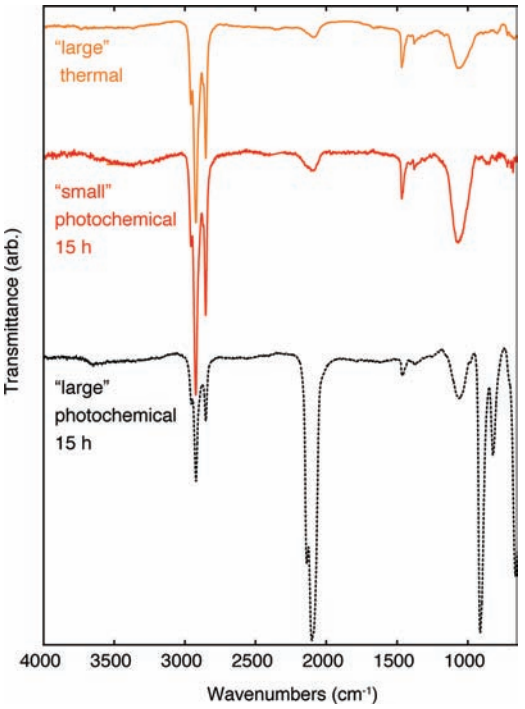


**Figure 1.** FTIR spectra of the "large" and "small" Si-NCs after thermal and photochemical reaction (orange and red traces) in comparison to the large Si-NCs after photochemical reaction (dashed black trace).

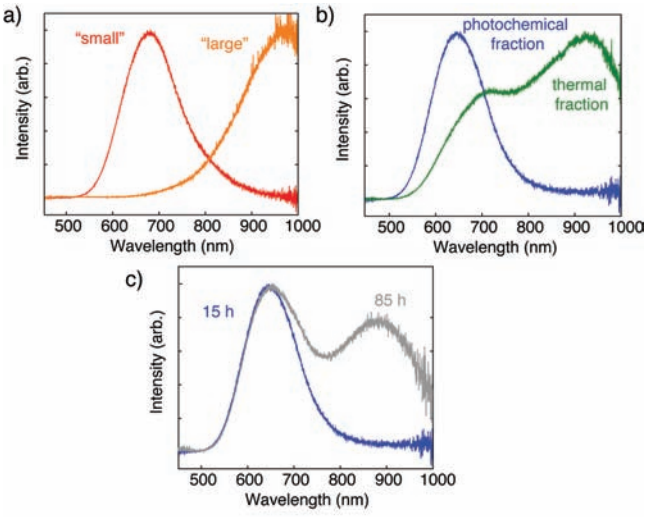


**Figure 2.** PL spectra of (a) "small" and "large" Si-NCs functionalized by photochemical and thermal hydrosilylation with 1-dodecene, respectively; (b) isolated fractions from sequential photochemical and thermal hydrosilylations with 1-dodecene with the "combined" Si-NC sample; (c) photochemical fractions of the "combined" Si-NC sample after 15 and 85 h.

PL in this spectral region have been successfully employed as *in vivo* luminescent tags with properties rivaling direct bandgap quantum dots.[35]

Initial attempts to functionalize larger Si-NCs (with PL centered at ca. 950 nm) with near-UV light were unsuccessful, yielding unreacted hydride-terminated Si-NCs as shown by FTIR spectroscopy in Figure 1; these Si-NCs exhibited poor dispersibility. Attempts to perform near-UV hydrosilylation with other larger sizes of Si-NCs that exhibit near-IR PL gave similar results. After 15 h of reaction, the FTIR spectrum is dominated by well-defined $Si-H_x$ stretching at ca. 2100 $cm^{-1}$ and scissoring at ca. 910 and 820 $cm^{-1}$. A small amount of oxidation is evidenced by Si−O−Si stretching at ca. 1100 $cm^{-1}$. Alkyl $\nu$ stretching at ca. 2900 $cm^{-1}$ and $\delta$ deformation bands at *ca.* 1460 and 1380 $cm^{-1}$ (attributed to residual hexane in the drop cast film analyzed, or possibly to a small degree of hydrosilylation) is also observed. In comparison, the equivalent photochemical reaction of "small" Si-NCs, or thermal hydrosilylation of "large" Si-NCs at 190 °C, resulted in a substantial decrease in $Si-H_x$ vibrations (accompanied with a broadening/red-shift of the $Si-H_x$ stretching vibrations), relative to the alkyl features. Correspondingly, the reaction mixtures turned from cloudy to clear as the Si-NCs became colloidally dispersed in neat 1-dodecene.

To better understand this difference in reactivity of various sizes of Si-NCs, photochemical hydrosilylation was attempted on a 10:1 "combined" mixture by mass of "small"/"large" Si-NCs. The size of the "large" sample (6.3 ± 1.0 nm as shown by SAXS below) was chosen as it straddles the Bohr radius of Si (ca. 5 nm), below which quantum confinement effects are expected to arise.[28]

Attempts to functionalize 1:1 and 5:1 "small"/"large" mixtures proved unsuccessful, resulting in hydride-terminated Si-NCs as indicated by FTIR (not shown). Two possible explanations could account for this observation. First, despite difficulties associated with quantitative study of Si-NC absorption cross sections arising from their indirect bandgap and relatively broad size distributions, Beard et al. have observed a substantial size dependence in the absorption cross-section of freestanding Si-NCs similar to the present samples.[46] These observations suggest absorption of near-UV light during the reaction is dominated by the "large" population, slowing the rate of functionalization of the "small" population. Second, efficient energy transfer from the "small" to "large" population could also hinder reactivity, especially if the NCs are in close proximity due to aggregation.[47]

Figure 2 shows photoluminescence of Si-NC samples after photochemical and/or thermal hydrosilylation with 1-dodecene. The "small" Si-NC sample exhibits PL centered at ca. 675 nm after photochemical reaction, in good agreement with previous *in situ* PL measurements;[30] the "large" Si-NC sample exhibits PL centered at ca. 950 nm after thermal hydrosilylation. After photochemical reaction, the "combined" sample was separated by centrifugation and filtration, resulting in PL centered at ca. 635 nm, blue-shifted compared to the small Si-NC sample. The residual precipitate from the photochemical reaction was redispersed in 1-dodecene and thermally functionalized, resulting in collodially dispersed Si-NCs exhibiting PL with two features centered at ca. 700 and 935 nm. Extending the photochemical reaction time and heating the reaction gently at 40 °C to increase the reaction rate (i.e., well below the threshold for thermal Si−H homolysis as discussed above) gave PL with two features centered at ca. 700 and 900 nm. The characteristic "small" PL was broadened in comparison to the 15 h reaction while the "large" PL was blue-shifted from the thermal reaction.

It is important to note that PL only probes the luminescent fraction of these samples, which are expected to contain a subpopulation of defect-ridden nonluminescent Si-NCs.[48] As well, PL spectroscopy could be affected by energy transfer process that further hinder quantitative interpretation of the observed size-dependent reactivity. To better understand the


dx.doi.org/10.1021/ja2025189 |*J. Am. Chem. Soc.* 2011, 133, 9564–9571

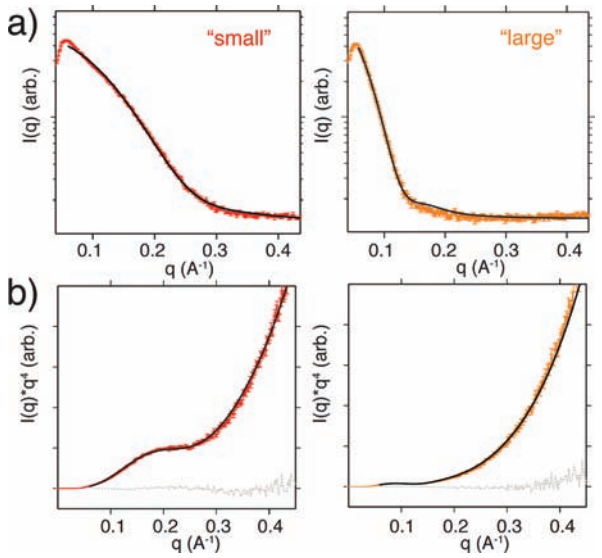


**Figure 3.** SAXS of "small" and "large" Si-NCs functionalized by photochemical and thermal hydrosilylation with 1-dodecene respectively: plotted as (a) $I(q)$ vs $q$ and (b) as a Porod plot with $I(q)\cdot q^4$ vs $q$. Fitting the data to a spherical particle model with a Gaussian distribution (fitting described in detail in Supporting Information, solid black line, residual shown in b as a dashed gray line) gave average nanocrystal diameters of 2.9 ± 0.6 and 6.3 ± 1.0 nm for the "small" and "thermal" samples, respectively.

size-dependent reactivity suggested by the PL results, the Si-NC samples were also characterized using SAXS, shown for the "small" and "large" Si-NCs in Figure 3. Compared to other techniques (e.g., atomic force microscopy or transmission electron microscopy, TEM), SAXS is a useful tool for rapid, quantitative determination of size and dispersity of nanomaterials, particularly for elements with low electron density contrast with carbon such as Si which can make TEM measurements very challenging.[31,49−52] Fitting the SAXS data in Figure 3 to a spherical particle model with a Gaussian distribution gave average nanocrystal diameters of 2.9 ± 0.6 and 6.3 ± 1.0 nm for the "small" and "large" samples, respectively, in good agreement with previous high resolution TEM[30] and X-ray diffraction analysis.[53]

The validity of the SAXS fitting approach for determining the relative concentrations of each population was verified by comparing results of mixtures of the "small" and "large" samples in known ratios (i.e., 1:2, 1:1, 10:1, and 25:1 "small"/ "large" mixtures, Figure S1 in Supporting Information). Fitting the SAXS data of the "combined" samples using the "small" and "large" populations revealed the relative volume fraction of each size in the aliquot of well-functionalized particles isolated after each functionalization (Figure 4). As mentioned above, the 10:1 mixture in the initial hydride-terminated reaction mixture contains approximately equal volume fractions of each population. After photochemical functionalization, the relative volume fraction of the "small" population was found to be 70%. The subsequent thermal hydrosilylation gave a "small" volume fraction of 24%. Increasing the photochemical reaction time from 15 to 85 h decreased the "small" volume fraction to 33%. However, it should be noted these fits assume the mean size of each population does not shift appreciably between the "combined" samples.

While the blue-shifted, slightly narrowed PL from the "combined" sample after 15 h of photochemical reaction is consistent with a shift in NC size, attempts to fit these data by allowing the size of each population to vary were unsuccessful. This may be due to the challenge of allowing too many parameters to vary during the fitting, or to the role of surface states in shifting the PL rather than solely size effects.[54]

Although the SAXS data suggest a significant volume of large Si-NCs in the 15 h photochemical aliquot, seemingly at odds with the PL results which show no PL from the large fraction, it is reasonable this could occur through a small number of the "large" Si-NCs reacting through an alternate free radical (nonsize dependent) pathway somewhat analogous to the decomposition-initiated pathway in thermal hydrosilylation observed by Mischki et al.[16] Recall, PL only probes the luminescent fraction, which are expected to be well-passivated and defect-free; it is reasonable a fraction of nonluminescent Si-NCs might contain a surface radical defect that could initiate this process. As well, it is important to note the total number of Si-NCs in the "combined" samples is always dominated by the "small" fraction, and thus, relatively few events occurring within the "large" fraction could conceivably skew the SAXS results owing to their larger volume per particle. The considerable difference in NC volume, the higher probability of the large NCs to contain volume defects,[55−57] and an extended chain length for the propagation reaction after relatively few initiation events[14] could all influence the increased volume fraction of the large population in the SAXS results.

The influence of size on the rate of the hydrosilylation of nanostructured Si surfaces using other initiation methods has been reported qualitatively. Hua et al. noted deep-UV hydrosilylation of Si-NCs exhibits a size dependence, based on the length of irradiation required for the dispersion to change from cloudy to clear.[58] This was attributed to the smaller NCs requiring a lower degree of alkyl grafting to produce stable colloidal dispersions. While this is an important consideration (along with the other factors mentioned above) for the present results, it cannot account for the size-dependent reactivity observed, as similar degrees of alkyl and hydride FTIR stretching features would be expected for the small and large 15 h photochemical samples.

This observed size-dependent reactivity is consistent with the calculations of Reboredo et al.,[26] who predicted that exciton-mediated hydrosilylation involves a metastable transition state forming a localized midgap state (not size-dependent). The formation of this transition state was predicted to be energetically favorable if the initial energy of the (photoexcited and thus size-dependent) reactants were high enough. This is consistent with the present observation that the large population requires longer irradiation times to produce colloidal, luminescent NCs.

In Stewart and Buriak's original report of exciton-mediated hydrosilylation, the reactivity was proposed to be limited to nanoscale Si on the basis of limited reactivity observed with nonluminescent porous Si samples.[20] However, only luminescent samples with PL centered at ca. 600−640 nm were investigated. The subsequent reports by Zuilhof and co-workers suggesting an exciton-mediated process initiated by visible light on bulk surfaces appears to conflict with Buriak's conclusion upon first inspection.[22−24] It is important to note (particularly for nanostructured Si surfaces) that while Si surfaces are known to share many common properties (e.g., low toxicity and possible biodegradation pathways),[32,33,35,59−62] they can exhibit substantial differences in surface chemistry, impurities, homogeneity,

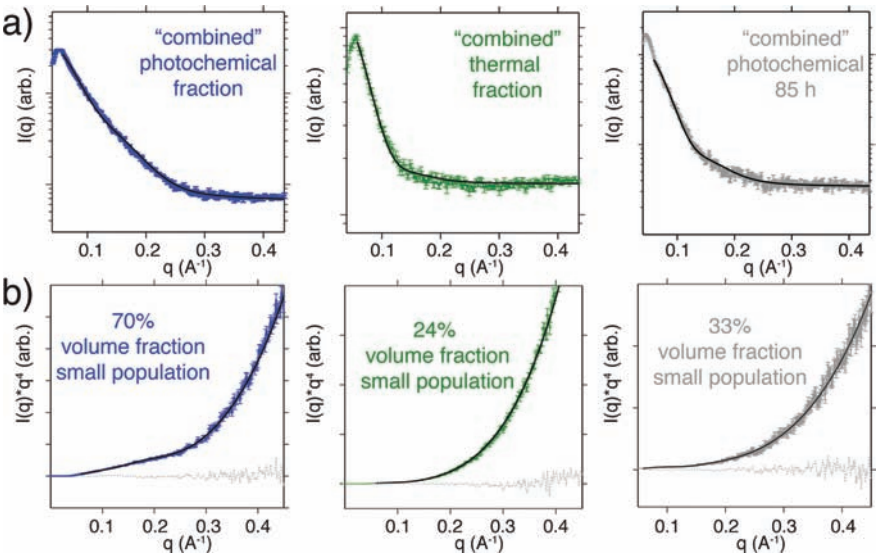


**Figure 4.** SAXS of fractions isolated from the "combined" sample after photochemical, thermal and extended photochemical hydrosilylation, plotted as (a) $I(q)$ vs $q$ and (b) as a Porod plot with $I(q) \cdot q^4$ vs $q$. The data was fit (solid black line, residual shown in b as a dashed gray line) to a combination of the populations obtained from SAXS of the "small" and "large" samples shown in Figure 3.

quantum size effects, etc. that could drastically influence the rate of hydrosilylation, and so a direct comparison between porous Si and the present freestanding Si-NCs may not be straightforward.

We previously demonstrated near-UV hydrosilylation with phenylacetylene produces colloidal, nonluminescent Si-NC dispersions. Phenylacetylene was previously observed to be unreactive in visible light hydrosilylation with porous Si by Stewart and Buriak. We originally attributed this difference to the 365 nm light source having sufficient energy to directly initiate hydride homolysis (i.e., following path A in Scheme 1).[30] In this mechanism, no size-dependent reactivity is expected, as the rate limiting step is direct photoinduced cleavage of the surface hydride.[7]

However, fitting SAXS data of a "combined" sample reacted photochemically for 15 h with phenylacetylene showed the same size-dependent reactivity observed with 1-dodecene, with a "small" Si-NC volume fraction of 69% (Figure 5). As these styrenyl-capped Si-NCs are nonluminescent, PL spectroscopy could not be used to assess the size-dependence of the reactivity. FTIR of the well-functionalized fraction (Figure S2 in Supporting Information) showed an increase in alkenyl stretching and decrease in hydride stretching features in comparison to nonfunctionalized NCs. Although the relative intensity of the hydride and oxide features is somewhat increased compared to the dodecyl-functionalized Si-NCs, suggesting a lower degree of surface coverage, this may also be due to the resulting smaller alkenyl group, decreased oscillator strength for alkene CH stretching vibrations compared to alkyl, or packing considerations of the surface styrenyl rings.[63,64]

The size-dependent reactivity observed with phenylacetylene implies an exciton-mediated mechanism rather than direct homolysis. Reaction with phenylacetylene quenches Si-NC PL, conflicting with the stipulations of Stewart and Buriak's nanoscale exciton-mediated mechanism (Path B, Scheme 1). They suggested a small number of phenylacetylene molecules would react and then trap excitons, preventing further reaction. However, phenylacetylene is expected to be reactive in Zuilhof's exciton-mediated mechanism (Path C) as excitons are only

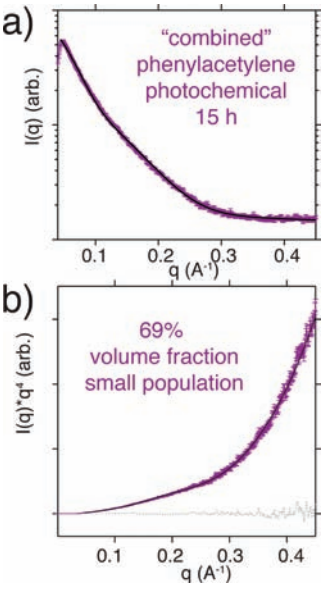


**Figure 5.** SAXS of the well-functionalized fraction isolated from the "combined" sample after photochemical hydrosilylation with phenylacetylene. Plotted as (a) $I(q)$ vs $q$ and (b) as a Porod plot with $I(q) \cdot q^4$ vs $q$. The data was fit (solid black line, residual shown in b as a dashed gray line) to a linear combination of the populations obtained from SAXS of the "small" and "large" samples shown in Figure 3.

involved in the initial nucleophilic attack, with radical propagation driving subsequent functionalization. Indeed, alkynes have been suggested to be more reactive in this pathway owing to their increased nucleophilicity and ability to stabilize radicals through delocalization over the resulting surface vinyl group.[23] The difference between Stewart and Buriak's results with phenylacetylene and the present observations might arise from the different absorption cross sections due to the irradiating wavelength, as near-UV light corresponds to a direct gap transition. As mentioned above, Kanai and Selloni suggested the radical

propagation in Path C is more favorable than hydride abstraction from the reactive site for bulk Si.[27] However, the intermediate and transition states for both paths involve highly localized electronic distortions, whereas the Si-NC electronic states are delocalized over the entire nanocrystal (and thus are sensitive to size). The same considerations for size-dependent reactivity predicted by Reboredo et al.[26] for Path B are therefore expected to hold for Path C, in keeping with the present observations.

## ■ CONCLUSIONS

In summary, we have demonstrated the influence of size on the reactivity of Si-NCs in near-UV hydrosilylation using PL, FTIR, and SAXS. These results are in keeping with the size-dependent reactivity predicted by theoretical studies of exciton-mediated mechanisms, with larger NCs reacting at a slower rate due to quantum size effects. Size-dependent reactivity was observed in hydrosilylation with both 1-dodecene and phenylacetylene, suggesting the exciton mechanisms may be dominant in near-UV initiation in either radical and nonradical hydrosilylation rather than direct hydride homolysis. Mechanistic considerations in the functionalization of Si-NCs by hydrosilylation could be important for selecting a set of reaction conditions for a desired Si-NC size and olefin to be grafted.

## ■ EXPERIMENTAL SECTION

**Chemicals.** HSQ (Dow Corning, trade name FOx-17, sold as a solution in methyl isobutyl ketone and toluene), 49% hydrofluoric acid (HF, J.T. Baker, electronics grade), and 95% ethanol (Sigma-Aldrich) were used as received. High-purity water (18.2 MΩ·cm) was obtained from a Barnstead Nanopure Diamond purification system. All other reagents were purchased from Sigma Aldrich as the highest purity available (95% or greater) and unless specified were used as received. Phenylacetylene and 1-dodecene were purified immediately before use by passing over neutral activated alumina to remove peroxide impurities.[65]

**Synthesis and Etching of Si-NCs.** Oxide-embedded Si-NC composites were prepared from HSQ as previously described.[43] Previous X-ray diffraction study has shown the formation of ca. 4 and 6 nm Si-NCs encapsulated in an silica matrix by processing at 1100 and 1200 °C, respectively.[53]

To produce freestanding hydride-terminated Si-NCs of different sizes, two different etching procedures were employed. To obtain Si-NCs with PL centered at ca. 650 nm, referred to as "small" Si-NCs (shown by previous electron microscopy to be ca. 2−3 nm),[30] a previously described etching procedure was used.[43] In brief, to 1 g of mechanically ground composite processed at 1100 °C in a Teflon beaker equipped with a stir bar was added 30 mL of a 1:1:1 solution of HF/ethanol/water. After 1 h of stirring, the dispersion changed color from brown to yellow.

To obtain Si-NCs with PL centered at ca. 950 nm, referred to as "large" Si-NCs (ca. 5−6 nm as shown below), 1 g of mechanically ground composite processed at 1200 °C was added to a Teflon beaker equipped with a stir bar along with 0.5 mL of concentrated HCl and 15 mL of HF. After 5 min of stirring, 7.5 mL of ethanol was added and the mixture stirred for an additional 5 min, yielding a cloudy brown dispersion.

Hydride-terminated Si-NCs were extracted from both etch mixtures using 2 aliquots of 15 mL of toluene.

**Size-Dependent Photochemical Functionalization.** Following extraction, 12.5 mL of the "small" and "large" extracts was transferred to centrifuge tubes along with a "combined" sample containing 12.5 mL of a 10:1 ratio by volume of the "small"/"large" toluene dispersions. Assuming the initial number of Si-NCs per gram is approximately constant for 1100−1200 °C-processed composites (reasonable given the dominant mechanism for Si-NC formation and growth has been shown to be diffusion of Si suboxide species through the matrix, rather than Ostwald ripening[53]), this should yield similar Si-NC concentrations for the "small" and "large" etches.

After centrifugation at 3000 rpm, the toluene was decanted and the precipitated hydride-terminated NCs were redispersed into the desired alkene mixture (25 mL of neat 1-dodecene or 25 mL of toluene and 4 mL of phenylacetylene). The mixtures were transferred into Schlenk flasks equipped with stir bars and quartz inserts for photochemical reaction under an argon atmosphere. The reaction mixtures were subjected to three freeze−pump−thaw cycles, and photochemical hydrosilylation was carried out using a 365 nm light source for 15 h as previously described.[30]

**Si-NC Purification.** Following photochemical functionalization, the reaction mixtures were transferred into centrifuge tubes and spun at 3000 rpm to precipitate any unreacted NCs. These precipitated NCs were washed three times with hexane, and could be reacted using a secondary thermal hydrosilylation, described below. The supernatant from each reaction was filtered through a 250 nm PTFE syringe filter into a 50 mL centrifuge tube. Dodecene-functionalized NCs were purified by precipitation by the addition of 37.5 mL of a 3:1 ethanol/methanol mixture and centrifugation (25 900 G), chosen due to the insolubility of dodecene in methanol. Three additional purification cycles by centrifugation were performed using toluene and methanol as the solvent/antisolvent.

To purify phenylacetylene-functionalized NCs, the majority of the toluene and phenylacetylene reaction mixture after filtration was removed under vacuum on a Schlenk line. The remaining concentrated mixture was subjected to three purification by centrifugation cycles using toluene and methanol as the solvent/antisolvent as described above.

**Thermal Hydrosilylation.** Hydride-terminated Si-NCs (either freshly HF etched or separated after photochemical functionalization) were dispersed in 25 mL of 1-dodecene and transferred to a Schlenk flask equipped with a stirbar under an argon atmosphere. The reaction mixture was degassed by three cycles of evacuation and purging with argon, after which the flask was placed in a silicon oil bath and heated at 190 °C for 15 h. The reaction mixture typically turned from turbid to transparent in the first 3 h of heating. Purification was carried out as described above.

**Characterization.** FTIR spectra were collected using a Nicolet Magna 750 IR spectrometer on drop-cast films. Photoluminescence spectra of dilute toluene Si-NC dispersions were excited with the 325 nm line of a He/Cd laser and collected using a fiber optic connected to an Ocean Optics USB2000 spectrometer. The spectrometer spectral response was normalized using a blackbody radiator. SAXS was performed on dilute dispersions of silicon nanocrystals in toluene sealed in a boron-rich silicate capillary (Charles Supper, 2 mm outer diameter, 80 mm length, 10 $\mu$m wall thickness). Measurements were performed using a Bruker NanoStar system with a rotating copper anode X-ray generator ($L$ = 1.54 Å) operating at 5.5 kW. The scattered photons were collected on a 2D multiwire gas-filled detector (Bruker Histar) and the scattering angle was calibrated using a silver behenate ($CH_3(CH_2)_{20}COOAg$) standard. Radial integrations of scattering intensity were performed using Bruker GADDS software. Experimental data were corrected for background scattering. SAXS data were fit to a standard model for a dilute dispersion of solid homogeneous spheres, described in detail in the Supporting Information.

Given the inherent variability in manually extracting the toluene dispersions from the etching mixture, a representative series of reactions prepared from the same batch of Si-NCs is described here. Each reaction was repeated a minimum of three times, and the variability of the "small"/"large" volume fractions obtained by SAXS was within 10%.

## ■ ASSOCIATED CONTENT

**Supporting Information.** Details of SAXS theory and fitting, SAXS fitting calibration curve and FTIR spectrum of Si-NCs functionalized with phenylacetylene. This material is available free of charge via the Internet at http://pubs.acs.org.

## ■ AUTHOR INFORMATION

**Corresponding Author**
jveinot@ualberta.ca

## ■ ACKNOWLEDGMENT

The authors acknowledge funding from the Natural Sciences and Engineering Research Council of Canada (NSERC), Canada Foundation for Innovation (CFI), Alberta Science and Research Investment Program (ASRIP), Alberta Innovates: Technology Futures, and University of Alberta Department of Chemistry. C. W. Moffat is thanked for assistance with FTIR characterization. S. Regli is thanked for assistance with PL characterization. S. Launspach is thanked for assistance with SAXS characterization. J. Rodríguez, M. Dasog, M. Johnson, and B. Benoit are thanked for useful discussions.

## ■ REFERENCES

(1) Linford, M. R.; Chidsey, C. E. D. *J. Am. Chem. Soc.* **1993**, *115*, 12631–12632.
(2) Buriak, J. M. *Chem. Rev.* **2002**, *102*, 1271–1308.
(3) Veinot, J. G. C. *Chem. Commun.* **2006**, 4160–4168.
(4) Ciampi, S.; Harper, J. B.; Gooding, J. J. *Chem. Soc. Rev.* **2010**, *39*, 2158–2183.
(5) Rosso-Vasic, M.; Spruijt, E.; Popović, Z.; Overgaag, K.; Van Lagen, B.; Grandidier, B.; Vanmaekelbergh, D.; Domínguez-Gutiérrez, D.; De Cola, L.; Zuilhof, H. *J. Mater. Chem.* **2009**, *19*, 5926–5933.
(6) Li, X.; He, Y.; Swihart, M. T. *Langmuir* **2004**, *20*, 4720–4727.
(7) Cicero, R. L.; Linford, M. R.; Chidsey, C. E. D. *Langmuir* **2000**, *16*, 5688–5695.
(8) Effenberger, F.; Götz, G.; Bidlingmaier, B.; Wezstein, M. *Angew. Chem., Int. Ed.* **1998**, *37*, 2462–2464.
(9) Boukherroub, R.; Morin, S.; Bensebaa, F.; Wayner, D. D. M. *Langmuir* **1999**, *15*, 3831–3835.
(10) Linford, M. R.; Fenter, P.; Eisenberger, P. M.; Chidsey, C. E. D. *J. Am. Chem. Soc.* **1995**, *117*, 3145–3155.
(11) Cicero, R. L.; Chidsey, C. E. D.; Lopinski, G. P.; Wayner, D. D. M.; Wolkow, R. A. *Langmuir* **2002**, *18*, 305–307.
(12) Lopinski, G. P.; Wayner, D. D. M.; Wolkow, R. A. *Nature* **2000**, *406*, 48–51.
(13) Chatgilialoglu, C.; Timokhin, V. I. *Adv. Organomet. Chem.* **2008**, *57*, 117–181.
(14) Woods, M.; Carlsson, S.; Hong, Q.; Patole, S. N.; Lie, L. H.; Houlton, A.; Horrocks, B. R. *J. Phys. Chem. B* **2005**, *109*, 24035–24045.
(15) Eves, B. J.; Lopinski, G. P. *Langmuir* **2006**, *22*, 3180–3185.
(16) Mischki, T. K.; Lopinski, G. P.; Wayner, D. D. M. *Langmuir* **2009**, *25*, 5626–5630.
(17) Wang, X.; Ruther, R. E.; Streifer, J. A.; Hamers, R. J. *J. Am. Chem. Soc.* **2010**, *132*, 4048–4049.
(18) Boukherroub, R.; Morin, S.; Wayner, D. D. M.; Bensebaa, F.; Sproule, G. I.; Baribeau, J. -M.; Lockwood, D. J. *Chem. Mater.* **2001**, *13*, 2002–2011.
(19) Coletti, C.; Marrone, A.; Giorgi, G.; Sgamellotti, A.; Cerofolini, G.; Re, N. *Langmuir* **2006**, *22*, 9949–9956.
(20) Stewart, M. P.; Buriak, J. M. *J. Am. Chem. Soc.* **2001**, *123*, 7821–7830.
(21) Sun, Q. -Y.; De Smet, L. C. P. M.; Van Lagen, B.; Giesbers, M.; Thüne, P. C.; Van Engelenburg, J.; De Wolf, F. A.; Zuilhof, H.; Sudhölter, E. J. R. *J. Am. Chem. Soc.* **2005**, *127*, 2514–2523.
(22) Scheres, L.; Arafat, A.; Zuilhof, H. *Langmuir* **2007**, *23*, 8343–8346.
(23) Scheres, L.; Giesbers, M.; Zuilhof, H. *Langmuir* **2010**, *26*, 10924–10929.
(24) Eves, B. J.; Sun, Q. -Y.; Lopinski, G. P.; Zuilhof, H. *J. Am. Chem. Soc.* **2004**, *126*, 14318–14319.
(25) Reed, C. A. *Acc. Chem. Res.* **1998**, *31*, 325–332.
(26) Reboredo, F. A.; Schwegler, E.; Galli, G. *J. Am. Chem. Soc.* **2003**, *125*, 15243–15249.
(27) Kanai, Y.; Selloni, A. *J. Am. Chem. Soc.* **2006**, *128*, 3892–3893.
(28) Cullis, A. G.; Canham, L. T.; Calcott, P. D. J. *J. Appl. Phys.* **1997**, *82*, 909–965.
(29) Wolkin, M. V.; Jorne, J.; Fauchet, P. M.; Allan, G.; Delerue, C. *Phys. Rev. Lett.* **1999**, *82*, 197–200.
(30) Kelly, J. A.; Veinot, J. G. C. *ACS Nano* **2010**, *4*, 4645–4656.
(31) Hessel, C. M.; Rasch, M. R.; Hueso, J. L.; Goodfellow, B. W.; Akhavan, V. A.; Puvanakrishnan, P.; Tunnel, J. W.; Korgel, B. A. *Small* **2010**, *6*, 2026–2034.
(32) Erogbogbo, F.; Yong, K.-T.; Roy, I.; Xu, G. X.; Prasad, P. N.; Swihart, M. T. *ACS Nano* **2008**, *2*, 873–878.
(33) Park, J. -H.; Gu, L.; von Maltzahn, G.; Ruoslahti, E.; Bhatia, S. N.; Sailor, M. J. *Nat. Mater.* **2009**, *8*, 331–336.
(34) Erogbogbo, F.; Yong, K. -T.; Hu, R.; Law, W. -C.; Ding, H.; Chang, C. -W.; Prasad, P. N.; Swihart, M. T. *ACS Nano* **2010**, *4*, 5131–5138.
(35) Erogbogbo, F.; Yong, K. −T.; Roy, I.; Hu, R.; Law, W. −C.; Zhao, W.; Ding, H.; Wu, F.; Kumar, R.; Swihart, M. T.; Prasad, P. N. *ACS Nano* **2011**, *5*, 413–423.
(36) Law, M.; Luther, J. M.; Song, Q.; Hughes, B. K.; Perkins, C. L.; Nozik, A. J. *J. Am. Chem. Soc.* **2008**, *130*, 5974–5985.
(37) Talapin, D. V.; Murray, C. B. *Science* **2005**, *310*, 86–89.
(38) Kovalenko, M. V.; Scheele, M.; Talapin, D. V. *Science* **2009**, *324*, 1417–1420.
(39) Cornelisse, J. *Chem. Rev.* **1993**, *93*, 615–669.
(40) Song, J. H.; Sailor, M. J. *J. Am. Chem. Soc.* **1997**, *119*, 7381–7385.
(41) Wang, D.; Buriak, J. M. *Langmuir* **2006**, *22*, 6214–6221.
(42) Content, S.; Trogler, W. C.; Sailor, M. J. *Chem.—Eur. J.* **2000**, *6*, 2205–2213.
(43) Hessel, C. M.; Henderson, E. J.; Veinot, J. G. C. *Chem. Mater.* **2006**, *18*, 6139–6146.
(44) Kelly, J. A.; Henderson, E. J.; Veinot, J. G. C. *Chem. Commun.* **2010**, *46*, 8704–8718.
(45) Weissleder, R. *Nat. Biotechnol.* **2001**, *19*, 316–317.
(46) Beard, M. C.; Knutsen, K. P.; Yu, P.; Luther, J. M.; Song, Q.; Metzger, W. K.; Ellingson, R. J.; Nozik, A. J. *Nano Lett.* **2007**, *7*, 2506–2512.
(47) Lockwood, R.; Hryciw, A.; Meldrum, A. *Appl. Phys. Lett.* **2006**, 89.
(48) Wilson, W. L.; Szajowski, P. F.; Brus, L. E. *Science* **1993**, *262*, 1242–1244.
(49) Choi, J.; Tung, S. -H.; Wang, N. S.; Reipa, V. *Nanotechnol.* **2008**, 19.
(50) Matsumoto, T.; Suzuki, J. -I.; Ohnuma, M.; Kanemitsu, Y.; Masumoto, Y. *Phys. Rev. B: Condens. Matter* **2001**, *63*, 1953221–1953225.
(51) Gracin, D.; Bernstorff, S.; Dubcek, P.; Gajovic, A.; Juraic, K. *J. Appl. Crystallogr.* **2007**, *40*, s373–s376.
(52) Bernstorff, S.; Dubček, P.; Kovačević, I.; Radić, N.; Pivac, B. *Thin Solid Films* **2007**, *515*, 5637–5640.
(53) Hessel, C. M.; Henderson, E. J.; Veinot, J. G. C. *J. Phys. Chem. C* **2007**, *111*, 6956–6961.
(54) Kelly, J. A.; Henderson, E. J.; Clark, R. J.; Hessel, C. M.; Cavell, R. G.; Veinot, J. G. C. *J. Phys. Chem. C* **2010**, *114*, 22519–22525.
(55) Cheylan, S.; Elliman, R. G. *Nucl. Instrum. Methods Phys. Res., Sect. B* **2001**, *175−177*, 422–425.

(56) Cheylan, S.; Elliman, R. G. *Appl. Phys. Lett.* **2001**, *78*, 1912–1914.
(57) Cheylan, S.; Elliman, R. G. *Appl. Phys. Lett.* **2001**, *78*, 1225–1227.
(58) Hua, F.; Swihart, M. T.; Ruckenstein, E. *Langmuir* **2005**, *21*, 6054–6062.
(59) Alsharif, N. H.; Berger, C. E. M.; Varanasi, S. S.; Chao, Y.; Horrocks, B. R.; Datta, H. K. *Small* **2009**, *5*, 221–228.
(60) Bayliss, S. C.; Heald, R.; Fletcher, D. I.; Buckberry, L. D. *Adv. Mater.* **1999**, *11*, 318–321.
(61) Nagesha, D. K.; Whitehead, M. A.; Coffer, J. L. *Adv. Mater.* **2005**, *17*, 921–924.
(62) Low, S. P.; Voelcker, N. H.; Canham, L. T.; Williams, K. A. *Biomaterials* **2009**, *30*, 2873–2880.
(63) Bateman, J. E.; Eagling, R. D.; Horrocks, B. R.; Houlton, A. *J. Phys. Chem. B* **2000**, *104*, 5557–5565.
(64) Sieval, A. B.; Vleeming, V.; Zuilhof, H.; Sudholter, E. J. R. *Langmuir* **1999**, *15*, 8288–8291.
(65) Jackson, H. L.; McCormack, W. B.; Rondestvedt, C. S.; Smeltz, K. C.; Viele, I. E. *J. Chem. Educ.* **1970**, *47*, A175–A188.